Quantum mechanical and quasiclassical simulations of molecular beam experiments for the $F+H_2 \rightarrow HF+H$ reaction on two *ab initio* potential energy surfaces

J. F. Castillo[a)]
Physical and Theoretical Chemistry Laboratory, South Parks Road, Oxford University, Oxford OX1 3QZ, United Kingdom

B. Hartke and H.-J. Werner
Institut für Theoretische Chemie, Universität Stuttgart, Pfaffenwaldring 55, D-70569 Stuttgart, Germany

F. J. Aoiz, L. Bañares, and B. Martínez-Haya
Departamento de Química Física, Facultad de Química, Universidad Complutense, 28040 Madrid, Spain

(Received 4 May 1998; accepted 29 July 1998)

Laboratory (LAB) angular distributions (AD) measured in molecular beam experiments by Lee and co-workers in 1985 and very recently by Keil and co-workers for the prototypic $F+H_2$ reaction have been simulated using new quantum mechanical (QM) and quasiclassical trajectory (QCT) state-resolved differential cross sections (DCS) calculated on the *ab initio* potential energy surfaces (PES) by Stark and Werner (SW) and by Hartke, Stark and Werner (HSW); the latter PES includes spin-orbit coupling corrections added to the entrance channel of the former. The simulations of the 1985 LAB ADs performed using the new QM calculations on the SW PES show a very good agreement with the experimental results for all final vibrational states of the HF product. The inclusion of spin-orbit coupling corrections in the *ab initio* HSW PES does not seem to improve the agreement between theoretical and experimental results. As for the simulation of the recent experiments of Keil and co-workers, the LAB ADs are very well reproduced by the QM and QCT results on both the SW and HSW PESs with the exception of the negative signal measured at LAB scattering angles of about $-8°$, arising from HF scattering into the forward hemisphere for the $v'=1$, $j'=5,6,7$ states. This peak cannot be accounted for by either of the QM and QCT calculations on any of the two PESs. © *1998 American Institute of Physics.* [S0021-9606(98)01241-0]

I. INTRODUCTION

In a recent work,[1] *ab initio* simulations of the 1985 molecular beam experiments of Lee and co-workers[2] for the $F+H_2$ reaction based on quantum mechanical (QM) and quasiclassical trajectory (QCT) calculations on the *ab initio* potential energy surface (PES) by Stark and Werner (hereafter SW)[3] were reported. The simulations using the QM differential cross sections (DCS) showed an unprecedentedly good agreement with the experimental results, consisting of laboratory (LAB) product angular distributions (AD) and time-of-flight (TOF) spectra. In particular, the height of the peak in the experimental LAB AD corresponding to HF ($v'=3$) forward scattering was quite well reproduced by the simulation using the QM theoretical results. The most important discrepancies between theory and experiment were found in the HF ($v'=3$) sideways and backward scattering. The simulations based on QCT data failed to account for most of the $v'=3$ forward scattering, although the backward scattering was very well accounted for. One of the main conclusions of this work was the importance of performing simulations of the experimental dynamical observables in the LAB system to assess the quality of a given calculation on a given PES.[1] In addition, it was suggested in that work that small adjustments of the PES, as, for example, the inclusion of spin-orbit effects, could yield to a very detailed agreement between theory and experiment.

However, the original experiments of Lee and co-workers had not enough resolution to yield information about rovibrational state-resolved DCSs. The availability of experimental v',j' integral and differential cross sections could provide a better means for the assessment of the *ab initio* PESs and the different dynamical calculations. Recently a considerable experimental effort has been spent in order to measure v',j' integral and differential cross sections for this system.[4–11]

The group of Toennies has investigated thoroughly the $F+D_2$ isotopic variant of the reaction at several collision energies,[4–8] using a conventional crossed molecular beam machine but with a resolution between three to four times higher than that of Neumark *et al.* From these experiments, vibrationally state-resolved DCSs[4–6] and absolute values of the total reaction cross section[7] as a function of collision energy were measured. Although no separated v',j' peaks could be resolved in the TOF spectra, a careful analysis of the envelopes allowed them to extract v',j' state-resolved DCSs in the center-of-mass (CM) frame.[8] These results have

[a)]Present address: Departamento de Química Física, Facultad de Química, Universidad Complutense, 28040 Madrid, Spain.

been compared with theoretical QM and QCT calculations performed on the SW PES,[6,8,12,13] yielding in general, a good concordance between theory and experiments.

Chapman *et al.*[9] have reported the measurement of the nascent rotational HF ($v'=3,j'$) distribution for the $F+H_2$ reaction using crossed-molecular beams and infrared (IR) direct absorption of the products at 1.8 kcal mol^{-1} collision energy. The experimental integral cross sections were compared with QM calculations carried out on the SW PES at 1.84 kcal mol^{-1} by Castillo and Manolopoulos. The most salient conclusion was that the experimental rotational distribution into $v'=3$ is hotter than the theoretical one, extending to higher j' values. One possible explanation given by the authors for the observed discrepancy was the contribution to reaction from a nonadiabatic channel involving $F(^2P_{1/2})$ atoms, which were also present in the atomic beam. On the other hand, the exothermicity for the $F+H_2$ reaction given by the SW PES is somewhat smaller than the experimental one,[3] and, therefore, the HF ($v'=3,j'$) product channels, which are energetically closed to reaction in the QM calculation, might be experimentally accessible at a given collision energy.

Keil and co-workers[10,11] have carried out new crossed-molecular beam experiments for the $F+H_2$ reaction. Angular distributions were measured for individual v',j' state-resolved states of HF by using IR laser excitation and bolometric detection of the products. The technique is sensitive to population differences between $v'=1,j'$ and $v'=2,j'-1$ HF states as a function of the LAB scattering angle. The measured LAB ADs were reproduced very well by simulations using QM v',j' state-resolved differential cross sections (DCS) calculated on the SW PES by Castillo and Manolopoulos. A very interesting feature in the experimental angular distributions was a negative bolometric signal at LAB scattering angles of $\approx -8°$ arising from HF ($v'=1,j'$) scattering in the forward hemisphere in the CM frame. This negative peak could be very well accounted for by the simulations with the QM state-resolved DCSs, and, in particular, it was found that the forward $v'=1$ products proceeds almost exclusively from reaction of fluorine atoms with H_2 molecules in initial $j=1$. Dharmasena *et al.* pointed out that since the QCT calculations of Aoiz *et al.*[14] on the same surface did not show appreciable scattering in the forward hemisphere for HF ($v'=1$), this feature might plausibly have a quantum mechanical origin.

In the meantime, Werner and co-workers have calculated a new *ab initio* PES for this system in which the spin-orbit correction in the entrance channel interaction has been included.[15] Using this PES, hereafter HSW, together with a new PES for the anionic FH_2^- species, Hartke and Werner[15] have performed time-dependent quantum mechanical simulations of the FH_2^- photoelectron spectra, which were shown to yield a better agreement with the high resolution photodetachment experimental results of Neumark and co-workers[16,17] than the previous ones using the SW PES.[18]

Prompted by the availability of all this experimental and theoretical information, we present in this work a new whole series of QM and QCT calculations on the SW PES, as well as on the new HSW PES for the $F+H_2(j=0-2)$ reaction at the collision energies corresponding to the experimental measurements of Neumark *et al.*[2] and Dharmasena *et al.*[10,11] Specifically, we have searched for the dynamical performance of the new HSW PES, and whether the new calculations could provide a better agreement with the experimental results. In addition, the convergence of the original QM calculations of Castillo *et al.*[19] has been improved in the present work by including more projections of the total angular momentum on the body-fixed frame z axis (the helicity). As a result of that, most of the oscillations found in the previously calculated v' state-resolved DCSs for the $F+H_2(j=1)$ reaction have disappeared in the new calculations. The new results for $j=0$ and $j=2$ are very similar to those reported in Ref. 19. The new QM and QCT theoretical calculations on the two PESs have been used to simulate the experimental LAB ADs of Neumark *et al.* and Dharmasena *et al.*

The paper is organized as follows: Sec. II gives a description of the methodology used for the QM and QCT calculations and for the simulations of the molecular beam experimental results. Section III contains the results of the QM and QCT calculations and the simulations and comparisons with the experimental angular distributions. The conclusions are summarized in Sec. IV.

II. METHOD

A. Potential energy surfaces

Two potential energy surfaces have been used in the present study: the previously reported *ab initio* SW PES[3] and a new PES based on the SW PES but with spin-orbit corrections added in the entrance channel (HSW PES). The spin-orbit (SO) matrix elements have been computed on the basis of the Breit–Pauli Hamiltonian using internally contracted multireference configuration interaction (MRCI) wave functions[20] for the lowest three electronic states which correlate with the $F(^2P)+H_2$ asymptote. All calculations were performed using the MOLPRO[21] *ab initio* program. In a diabatic representation,[3] the SO matrix elements were found to be virtually independent of the bending angle and, therefore, it was sufficient to compute them for linear geometries. The angle-dependent adiabatic PESs were obtained by diagonalizing the total Hamiltonian $H_{el}^{\mathrm{dia}}(R,r,\gamma)+H_{\mathrm{SO}}^{\mathrm{dia}}(R,r)$ with the assumption that $H_{\mathrm{SO}}^{\mathrm{dia}}(R,r)$ is independent of γ (R is the distance between the F atom and the H_2 center of mass, r the distance between the two H atoms, and γ the angle between the corresponding vectors **R** and **r**). The spin-orbit correction for the electronic ground state was spline fitted and then added to the SW PES fit. Since the SO correction is very small in the barrier region,[3] but lowers the asymptotic $F(^2P_{3/2})+H_2$ state by one third of the SO splitting of the fluorine atom, the barrier height is increased by approximately 0.38 kcal/mol. A comparison of the stationary point properties of the SW and HSW PESs is given in Table I. Obviously, the only larger differences between the two surfaces are in the barrier height (not in its location) and in the location of the van der Waals well in the entrance channel. The latter difference, however, is not a significant feature of the *ab initio* data, since both surfaces are very flat in this region, and hence small deviations and artifacts of the fit and

TABLE I. Stationary points on the SW and HSW PESs.

Surface	R_{HF}[a]	R_{HH}[a]	E[b]	Θ[c]
Collinear barrier				
SW[d]	2.950	1.442	1.92	0
HSW	2.947	1.442	2.29	0
Bent barrier				
SW[d]	2.922	1.457	1.53	61
HSW	2.914	1.458	1.91	62
Well depth in the entrance channel				
SW[d]	4.89	1.40	0.37	90
HSW	5.39	1.41	0.18	90
Well depth in the exit channel				
SW[d]	4.19	1.74	0.25	0
HSW	4.19	1.74	0.25	0

[a]Bond distance in bohr.
[b]Energies in kcal/mol.
[c]Bending angles in degree. As in Ref. 3, for both barriers, 180°-Θ is the FHH bond angle, while for the wells, Θ is the angle coordinate in the corresponding $F+H_2$ and $H+FH$ systems, respectively.
[d]Reference 3.

the spline interpolation easily lead to differences of this magnitude. Both PESs (SW and HSW) used in this work are available from the authors upon request.[22]

B. Quantum mechanical and quasiclassical trajectory calculations

The QM and QCT calculations have been performed for the $F+H_2(v=0, j=0-2)$ reaction on both the SW and HSW PESs at collision energies 79 meV (1.84 kcal mol^{-1}), 119 meV (2.74 kcal mol^{-1}), 148 meV (3.42 kcal mol^{-1}), and 160 meV (3.69 kcal mol^{-1}); the first three energies correspond to the collision energies of the experiment of Neumark *et al.*,[2] whereas the latter is the mean collision energy of the recent experiment of Dharmasena *et al.*[10,11]

The present quantum reactive scattering calculations were performed using the CCP6 quantum reactive scattering program,[23] which uses the same coupled-channel hyperspherical coordinate method employed in our previous study of the $F+H_2$ reaction.[19] In order to simulate the $F+H_2$ molecular beam experiments, it is necessary to perform calculations for a large number of total angular momenta, triatomic parity blocks, H_2 permutation symmetry blocks, and total energies. The three key convergence parameters in our coupled-channel hyperspherical coordinate program are denoted E_{max}, j_{max}, and k_{max}. The first two parameters define the coupled-channel basis set, which contains all $F+H_2$ and $HF+H$ channels with diatomic energy levels less than or equal to E_{max} and rotational quantum number less than or equal to j_{max}. We have performed convergence tests for vibrationally state-resolved reaction probabilities for the $F+H_2(v=0, j=0,1,2)$ reactions as a function of E_{max} and j_{max} at the four collision energies considered in this work, and total angular momentum $J=0$. It was found that reaction probabilities are all well converged using $E_{max}=1.4$ eV and $j_{max}=16$ on both SW and HSW PESs.

The convergence parameter k_{max} is only relevant for total angular momenta $J>0$, where it serves as an upper limit on the helicity quantum number k. In Ref. 19, the convergence of the reactive scattering probabilities as a function of k_{max} at the three collision energies of the experiments of Lee and co-workers and $J=14$ was examined. At this value of J, the total opacity function $(2J+1)P^J$ has its maximum value at $E_{coll}=148$ meV (3.42 kcal mol^{-1}). It was found that the reaction probabilities were all well converged by retaining angular basis functions with all allowed helicity quantum numbers in the $F+H_2$ reactant arrangement, $k_{max}=16$, and basis functions with helicities up to $k_{max}=4$ in the $HF+H$ product arrangement. In the present work, it has been found that precisely the same results are obtained using $k_{max}=4$ for both reactant and products channels, and all the calculations have been performed using the same k_{max} for the two arrangements. In addition, the convergence tests carried out in the present calculations on the SW and HSW PESs indicate that whereas a value of $k_{max}=5$ gave the same reaction probabilities as $k_{max}=4$ with differences smaller than 1%, the computed DCSs, especially those for $F+H_2(j=1)$, proved to be very sensitive to the value of k_{max}. For instance, the visible oscillations that were present in the reported v' state-resolved DCSs of Ref. 19 disappear when using $k_{max}=5$. Another difference, relevant for the comparison with the experimental results of Dharmasena *et al.* (see below), was the noticeable decrease of scattering into the forward hemisphere for HF ($v'=1$) products, specifically for $j'>4$. To further check the convergence, calculations have been carried out at the highest collision energy with $k_{max}=6$, and the DCSs were indistinguishable from the ones obtained using $k_{max}=5$, and in particular those for products into $v'=1$. Therefore, the production parameters for the present calculations are, $E_{max}=1.4$ eV, $j_{max}=16$, and $k_{max}=5$. It results in a coupled-channel basis set containing a total of 134 channels for $J=0$, for $J\geqslant 5$, there are up to 664 channels for $H_2(v=0, j=0)$, 531 channels for $H_2(v=0, j=1)(-1)^J=1$, 663 channels for $H_2(v=0, j=1)(-1)^J=-1$, 530 channels for $H_2(v=0, j=2)(-1)^J=1$, and 664 channels for $H_2(v=0, j=2)(-1)^J=-1$. Calculations up to $J=25$ were needed to get converged DCSs.

The general method for the calculation of quasiclassical trajectories is the same as the one used in previous works (see Refs. 12 and 24). Batches of 100 000 trajectories have been calculated at each collision energy and initial rotational quantum number on each of the two PESs. The main difference of the present calculations, with respect to those carried out previously on the SW PES,[14] is the quantization of the initial rotational angular momentum of the H_2 molecule. In previous work,[14] the square of the rotational angular momentum was equated to $j(j+1)\hbar^2$; thus, for $j=0$ the molecule had absolutely no rotational motion. However, Azriel *et al.*[25] pointed out that the use of the semiclassical quantization resulting from replacing $j(j+1)\hbar^2$ by $(j+1/2)^2\hbar^2$ (known as Langer correction), produces a somewhat better agreement with exact QM calculations. In fact, we have observed that the inclusion of a ''residual'' rotation in $j=0$ improves the agreement not only with QM calculations, but also with experimental results, especially in the case of the SW PES.[12] Therefore, in the present case, we have adopted such quantization, which, as a matter of fact, is only important for the

reaction with H_2 in $j=0$. In order to use an equivalent assignment method for reagents and products, the quantization is carried out in such a way that for a given initial quantum number, j, the value of the modulus of the rotational angular momentum has been randomly (uniformly) chosen in the range $[j\hbar,(j+1)\hbar]$. In any case, the results are practically the same if the initial modulus is kept fixed to $(j+1/2)\hbar$ for all the trajectories. This quantization scheme has been used also for the assignment of products' quantum numbers, which is carried out by equating the modulus of the classical HF molecule rotational angular momentum to $(j'+1/2)\hbar$. With the (real) j' value so obtained, the vibrational quantum number v' is found by equating the internal energy of the outgoing molecule to a rovibrational Dunham expansion (containing 20 terms) calculated by fitting the rovibrational energies given by the asymptotic diatomic limits of the SW or HSW PES. The values of v' and j' found in this way are then rounded to the nearest integer. It should be noticed that for both the H_2 and HF molecules the rovibrational levels have been calculated using the actual potential of the corresponding PES instead of using the experimental values.

As in previous work, the v',j' state-resolved DCSs are obtained by the method of moments expansion in Legendre polynomials. The Smirnov–Kolmogorov test was used to decide when to truncate the series. The QCT reaction probabilities as a function of total angular momentum were also calculated using this same method. For more details see Ref. 24.

C. Simulation of laboratory angular distributions

The simulation of the LAB ADs has been performed using the same methodology presented elsewhere.[1,5,12,26] As mentioned above, the experiments to be considered here are those of Neumark *et al.*,[2] performed with continuous molecular beams and mass spectrometric product detection, and those of Keil and co-workers,[10,11] where the products were detected by IR laser excitation in conjunction with bolometric detection. In the latter case, the technique is sensitive to flux differences between $v'=1,j'$ and $v'=2,j'-1$ states. Therefore, in this case, the measured LAB AD corresponds to the difference between scattering into two different rovibrational states. Whereas these measurements do not allow by themselves the extraction of individual CM v',j' DCSs they are ideally suited for a test based on the precise simulation of the experiment using theoretical v',j' state-resolved DCSs. In all cases, the simulations have been performed using the new QM and QCT v',j' state-resolved DCSs calculated on both the SW and HSW PESs.

The simulation of the LAB ADs from the experiments of Neumark *et al.*[2] is carried out by transforming the theoretical CM v',j' DCSs into the LAB system, and performing the convolution with the experimental distributions of beam velocities and divergences and detector aperture. The relevant equations, methodology, and experimental parameters can be found in Ref. 1.

In the case of the experiment of Dharmasena *et al.*,[10,11] the reported LAB ADs, $P_{\mathrm{diff}}(\Theta_{\mathrm{LAB}})$, correspond to the differences in bolometric signal with laser off and laser on, and thus, for each Θ_{LAB},

$$P_{\mathrm{diff}}=P_{\mathrm{off}}-P_{\mathrm{on}}=(N_2G_1-N_1G_2)\Delta E, \tag{1}$$

where ΔE is the difference of internal energy of the upper (2) and lower (1) v',j' states involved, and $G_1=g_1/(g_1+g_2)$ and $G_2=g_2/(g_1+g_2)$ are the corresponding rotational degeneracy factors giving relative populations under saturation conditions.[11]

The flux of molecules into the lower and upper v',j' states as a function of Θ_{LAB}, N_1, and N_2, respectively, is given by

$$N_i(\Theta_{\mathrm{LAB}})=\sum_j P(j)\int d^3\mathbf{r}n_1(\mathbf{r})n_2(\mathbf{r})\int d\ \Omega\ D(\Omega,\Theta_{\mathrm{LAB}}) \times\int\int dv_1dv_2\ f(v_1)f(v_2)\cdot v_r\cdot\sum_{q=1,2}\left(\frac{d^2\sigma}{d\omega}\right)_{iq} \cdot\frac{v_{iq}^2}{w_i^2\cos\xi_{iq}}. \tag{2}$$

The different integrals are performed by a Monte Carlo sampling of the reagent beam velocities v_1 and v_2 with distributions $f(v_1)$ and $f(v_2)$, and spatial beam densities $n_1(\mathbf{r})$ and $n_2(\mathbf{r})$, where the position vector $\mathbf{r}$ refers to a point in the scattering volume defined by the beam divergences and the geometry of the experiment as given in Ref. 11. In this equation, v_r is the relative velocity, v_{iq} and w_i are the LAB and CM velocities of the ith HF state, respectively, and ξ_{iq} is the angle between v_{iq} and w_i. The summation over $q=1,2$ takes into account the fact that, for a given quantum state of the products, there might be, at a given Θ_{LAB}, both fast and slow products in the LAB system. Notice that in this experiment, the detected signal is proportional to the flux of the HF product. The $D(\Omega,\Theta_{\mathrm{LAB}})$ factor accounts for the cone of acceptance of the detector and was determined from the geometry of the experiment. The experimental parameters for the simulation have been directly taken from Table I of Ref. 11.

The results of the different simulations have been obtained by appropriately weighting on the initial rotational quantum number j of the H_2 reagent, as indicated in Eq. (2) via the summation over j. The corresponding weights for the experiment of Neumark *et al.*, $P(j=0,1,2)$, are exactly the same as the ones listed in Table I of Ref. 1. The H_2 rotational temperature for the experiment of Dharmasena *et al.* has been obtained by linear interpolation of previously measured rotational populations of H_2 molecules in supersonic beams[27] under similar expansion conditions, and is estimated to be $T_{\mathrm{rot}}=115$ K, which gives a population of $\sim 25\%$ for $j=0$ and 75% for $j=1$.

The scaling factor between experiment and simulation for the experiments of Neumark *et al.* was obtained by performing a least squares fit of the corresponding LAB AD in order to minimize the difference between the theoretically calculated and measured data (see Ref. 1). In the case of the experiment of Dharmasena *et al.*, following Ref. 11, each LAB AD was independently normalized at the reference angle $\Theta_{\mathrm{LAB}}=14°$.

TABLE II. QM and QCT vibrationally state-resolved integral cross sections ($Å^2$) for the $F+H_2(v=0, j=0-2)\rightarrow HF+H$ reaction at the collision energy of 1.84 kcal mol^{-1} (78.9 meV) calculated on the SW and HSW PESs. Values in parentheses are the branching ratios defined as $\sigma_R(v')/\sigma_R(v'=2)$.

Surface	Method	$v'=1$	$v'=2$	$v'=3$	all v'
SW PES	QCT ($j=0$)	0.44 (0.19)	2.35 (1.0)	1.20 (0.51)	3.99
	QM ($j=0$)	0.63 (0.18)	3.48 (1.0)	1.35 (0.39)	5.46
HSW PES	QCT ($j=0$)	0.13 (0.09)	1.41 (1.0)	0.84 (0.60)	2.38
	QM ($j=0$)	0.28 (0.13)	2.16 (1.0)	1.07 (0.50)	3.51
SW PES	QCT ($j=1$)	0.54 (0.19)	2.91 (1.0)	1.57 (0.54)	5.02
	QM ($j=1$)	0.55 (0.16)	3.47 (1.0)	1.62 (0.47)	5.64
HSW PES	QCT ($j=1$)	0.20 (0.11)	1.78 (1.0)	1.19 (0.67)	3.17
	QM ($j=1$)	0.34 (0.13)	2.54 (1.0)	0.90 (0.35)	3.78
SW PES	QCT ($j=2$)	0.66 (0.23)	2.86 (1.0)	2.11 (0.74)	5.63
	QM ($j=2$)	0.77 (0.24)	3.22 (1.0)	1.92 (0.60)	5.91
HSW PES	QCT ($j=2$)	0.35 (0.18)	1.97 (1.0)	1.45 (0.74)	3.77
	QM ($j=2$)	0.49 (0.21)	2.33 (1.0)	1.17 (0.50)	3.99
SW PES	QCT (p-H_2)	0.48 (0.20)	2.45 (1.0)	1.38 (0.56)	4.05
	QM (p-H_2)	0.66 (0.19)	3.43 (1.0)	1.46 (0.43)	5.55
HSW PES	QCT (p-H_2)	0.17 (0.11)	1.52 (1.0)	0.96 (0.63)	2.65
	QM (p-H_2)	0.32 (0.15)	2.19 (1.0)	1.09 (0.50)	3.60
SW PES	QCT (n-H_2)	0.53 (0.19)	2.80 (1.0)	1.53 (0.54)	4.86
	QM (n-H_2)	0.58 (0.17)	3.46 (1.0)	1.58 (0.46)	5.62
HSW PES	QCT (n-H_2)	0.20 (0.12)	1.72 (1.0)	1.14 (0.66)	3.06
	QM (n-H_2)	0.34 (0.14)	2.45 (1.0)	0.95 (0.39)	3.74
Experiment	p-H_2	(0.20)	(1.0)	(0.68)	
	n-H_2	(0.21)	(1.0)	(0.67)	

In order to check for the reliability of the method, the experimental LAB ADs of Refs. 10 and 11 were simulated with precisely the same theoretical[19] CM v',j' state-resolved DCSs as those employed by Dharmasena *et al.*, obtaining exactly the same results as in Refs. 10 and 11.

III. RESULTS AND DISCUSSION

Tables II–IV list the QM and QCT v' state-resolved and total reaction cross section for the $F+H_2(j=0-2)$ reaction calculated on both the SW and HSW PESs at the collision energies of the experiment of Neumark *et al.* The corresponding values weighted on initial j according to the experimental H_2 rotational distribution (see Table I of Ref. 1) for the $p-H_2$ and $n-H_2$ molecular beams are also included. The values in parentheses correspond to the experimental and theoretical branching ratios defined as $\sigma_R(v')/\sigma_R(v'=2)$. The QCT total reaction cross sections are, in general, smaller than the QM ones for a given PES and the differences are larger for initial $j=0$ than for $j=1$ and $j=2$. As for the comparison between the calculations on the SW vs the HSW PES, the QM and QCT reaction cross sections calculated on the former are always significantly larger than those calculated on the latter, in accordance with the higher barrier of the HSW PES. In general, the agreement between

TABLE III. QM and QCT vibrationally state-resolved integral cross sections ($Å^2$) for the $F+H_2(v=0, j=0-2)\rightarrow HF+H$ reaction at the collision energy of 2.74 kcal mol^{-1} (119 meV) calculated on the SW and HSW PESs. Values in parentheses are the branching ratios defined as $\sigma_R(v')/\sigma_R(v'=2)$.

Surface	Method	$v'=0$	$v'=1$	$v'=2$	$v'=3$	all v'
SW PES	QCT ($j=0$)	0.03 (0.01)	1.51 (0.50)	3.00 (1.0)	0.97 (0.32)	5.51
	QM ($j=0$)	0.08 (0.02)	1.20 (0.26)	4.60 (1.0)	0.81 (0.18)	6.69
HSW PES	QCT ($j=0$)	⋯	0.99 (0.39)	2.55 (1.0)	0.90 (0.35)	4.44
	QM ($j=0$)	0.05 (0.01)	0.86 (0.23)	3.81 (1.0)	0.79 (0.21)	5.51
SW PES	QCT ($j=1$)	0.03 (0.01)	1.14 (0.31)	3.66 (1.0)	1.77 (0.48)	6.60
	QM ($j=1$)	0.08 (0.02)	1.08 (0.26)	4.12 (1.0)	1.76 (0.43)	7.04
HSW PES	QCT ($j=1$)	⋯	0.76 (0.26)	2.97 (1.0)	1.59 (0.54)	5.32
	QM ($j=1$)	0.05 (0.01)	0.74 (0.21)	3.46 (1.0)	1.51 (0.44)	5.76
SW PES	QCT ($j=2$)	0.05 (0.01)	1.09 (0.31)	3.55 (1.0)	2.45 (0.69)	7.14
	QM ($j=2$)	0.08 (0.02)	1.10 (0.28)	3.86 (1.0)	2.33 (0.60)	7.37
HSW PES	QCT ($j=2$)	0.02 (0.01)	0.79 (0.27)	2.96 (1.0)	2.05 (0.69)	5.82
	QM ($j=2$)	0.06 (0.02)	0.82 (0.25)	3.23 (1.0)	1.92 (0.59)	6.03
SW PES	QCT (n-H_2)	0.03 (0.01)	1.19 (0.34)	3.54 (1.0)	1.76 (0.50)	6.52
	QM (n-H_2)	0.08 (0.02)	1.10 (0.27)	4.15 (1.0)	1.71 (0.41)	7.04
HSW PES	QCT (n-H_2)	⋯	0.80 (0.27)	2.91 (1.0)	1.56 (0.54)	5.27
	QM (n-H_2)	0.05 (0.01)	0.77 (0.22)	3.48 (1.0)	1.47 (0.42)	5.77
Experiment	n-H_2		(0.23)	(1.0)	(0.53)	

TABLE IV. QM and QCT vibrationally state-resolved integral cross sections (Å^2) for the F+H$_2$($v=0$, $j=0-2$)→HF+H reaction at the collision energy of 3.42 kcal mol^{-1} (148 meV) calculated on the SW and HSW PESs. Values in parentheses are the branching ratios defined as $\sigma_R(v')/\sigma_R(v'=2)$.

Surface	Method	$v'=0$	$v'=1$	$v'=2$	$v'=3$	all v'
SW PES	QCT ($j=0$)	0.17 (0.05)	2.00 (0.65)	3.09 (1.0)	0.88 (0.28)	6.14
	QM ($j=0$)	0.13 (0.03)	1.60 (0.34)	4.65 (1.0)	0.66 (0.14)	7.02
HSW PES	QCT ($j=0$)	0.06 (0.02)	1.60 (0.58)	2.77 (1.0)	0.81 (0.29)	5.24
	QM ($j=0$)	0.09 (0.02)	1.19 (0.28)	4.22 (1.0)	0.60 (0.14)	6.10
SW PES	QCT ($j=1$)	0.09 (0.02)	1.58 (0.42)	3.77 (1.0)	1.68 (0.45)	7.12
	QM ($j=1$)	0.12 (0.03)	1.41 (0.33)	4.34 (1.0)	1.66 (0.38)	7.53
HSW PES	QCT ($j=1$)	0.04 (0.01)	1.19 (0.36)	3.34 (1.0)	1.56 (0.47)	6.13
	QM ($j=1$)	0.09 (0.02)	1.09 (0.28)	3.85 (1.0)	1.48 (0.38)	6.51
SW PES	QCT ($j=2$)	0.10 (0.03)	1.34 (0.36)	3.77 (1.0)	2.48 (0.66)	7.69
	QM ($j=2$)	0.12 (0.03)	1.35 (0.33)	4.06 (1.0)	2.36 (0.58)	7.89
HSW PES	QCT ($j=2$)	0.06 (0.02)	1.05 (0.32)	3.30 (1.0)	2.21 (0.67)	6.63
	QM ($j=2$)	0.09 (0.02)	1.09 (0.31)	3.56 (1.0)	2.08 (0.58)	6.82
SW PES	QCT (n-H$_2$)	0.10 (0.03)	1.57 (0.43)	3.69 (1.0)	1.78 (0.48)	7.14
	QM (n-H$_2$)	0.12 (0.03)	1.42 (0.33)	4.31 (1.0)	1.71 (0.40)	7.56
HSW PES	QCT (n-H$_2$)	0.05 (0.01)	1.21 (0.37)	3.26 (1.0)	1.63 (0.50)	6.15
	QM (n-H$_2$)	0.09 (0.02)	1.10 (0.29)	3.82 (1.0)	1.52 (0.40)	6.53
Experiment	n-H$_2$		(0.33)	(1.0)	(0.48)	

experimental and theoretical branching ratios is qualitative and tends to improve when the calculations are performed on the new HSW PES. The experimental $v'=1/v'=2$ branching ratios at the different collision energies are somewhat better reproduced by the QM calculations on the HSW PES, whereas the best agreement for the $v'=3/v'=2$ branching ratios are obtained for the QCT calculations on the HSW PES. The QM $v'=3/v'=2$ branching ratios calculated on both the SW and HSW PESs are somewhat smaller than the experimental ones and much less sensitive to the collision energy. The QM and QCT v' state-resolved and total reaction cross sections for the title reaction at the higher collision energy of 3.69 kcal mol^{-1} (160 meV), corresponding to the average collision energy of the experiments of Dharmasena *et al.*, are listed in Table V. The same trends discussed above for the QM and QCT total reaction cross sections calculated on the two PESs are obtained also at this collision energy.

Figures 1 and 2 display QM and QCT vibrational state-resolved DCSs calculated at the collision energies and with the initial rotational distributions of the experiment of Neumark *et al.*[2] on the SW and HSW PESs, respectively. The main difference between the present QM DCSs calculated on the SW PES (see Fig. 1) and those previously reported in Ref. 19 proceeds mainly from the calculations for $j=1$, which, as commented on above, were found to be not fully converged. As a result of that, the oscillations obtained on the v' state-resolved, especially at the highest collision energies (see Figs. 1 and 2 of Ref. 19), have disappeared in the present calculations. In addition, forward and sideways scattering into $v'=1$ and $v'=2$ have decreased substantially, whereas the forward peak into $v'=3$ has slightly increased. In the case of the QCT calculations, the slight differences of the present QCT DCSs calculated on the SW PES in comparison with the ones reported in Ref. 14 are almost exclusively due to the calculations for $j=0$, as a consequence of using the $(j+1/2)^2\hbar^2$ quantization rule for the initial rotational angular momentum in the present case.

The most evident difference between the present QM and QCT DCSs calculated on both PESs is the size of the forward peak into $v'=3$ and, to a lesser extent, into $v'=2$, as it has been discussed in previous work.[19,28] The scattering into the forward hemisphere is in general underestimated in

TABLE V. QM and QCT vibrationally state-resolved integral cross sections (Å^2) for the F+H$_2$($v=0$, $j=0-2$)→HF+H reaction at the collision energy of 3.69 kcal mol^{-1} (160 meV) calculated on the SW and HSW PESs.

Surface	Method	$v'=0$	$v'=1$	$v'=2$	$v'=3$	all v'
SW PES	QCT ($j=0$)	0.21	2.16	3.15	0.81	6.33
	QM ($j=0$)	0.15	1.71	4.71	0.63	7.20
HSW PES	QCT ($j=0$)	0.11	1.80	2.82	0.75	5.48
	QM ($j=0$)	0.11	1.35	4.27	0.58	6.31
SW PES	QCT ($j=1$)	0.11	1.70	3.81	1.65	7.27
	QM ($j=1$)	0.14	1.52	4.45	1.60	7.71
HSW PES	QCT ($j=1$)	0.07	1.36	3.40	1.54	6.37
	QM ($j=1$)	0.10	1.22	3.97	1.47	6.76
SW PES	QCT ($j=2$)	0.12	1.43	3.82	2.48	7.85
	QM ($j=2$)	0.16	1.45	4.14	2.36	8.11
HSW PES	QCT ($j=2$)	0.08	1.18	3.40	2.24	6.90
	QM ($j=2$)	0.11	1.20	3.69	2.12	7.12

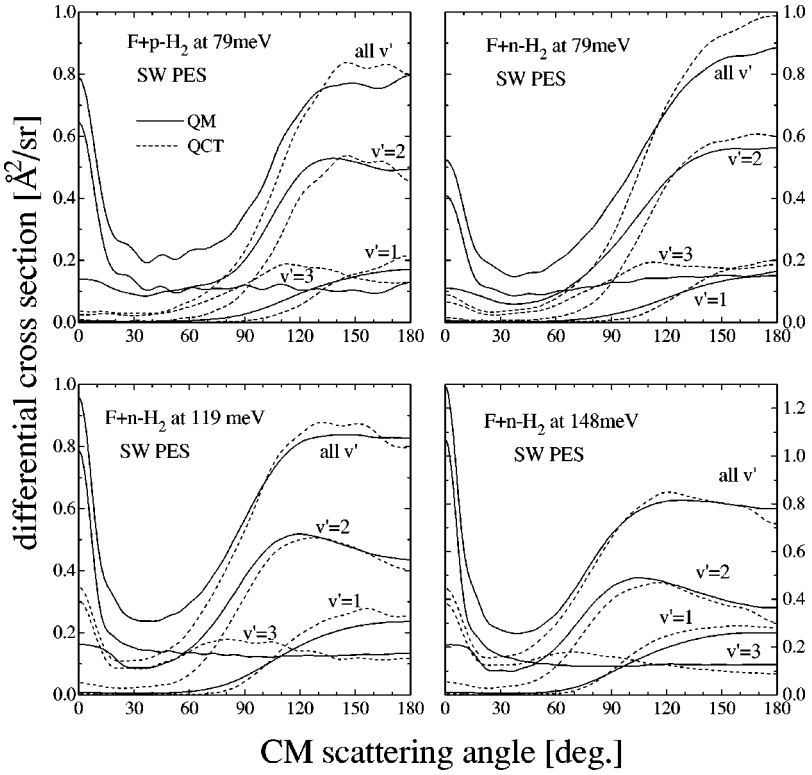

FIG. 1. QM (solid lines) and QCT (dashed lines) v' state-resolved DCSs for the $F+p-H_2$ reaction at 79 meV collision energy and for the $F+n-H_2$ reaction at 79, 119, and 148 meV collision energies calculated on the SW PES and weighted on initial j as in Ref. 1.

the QCT calculations, since it is related to tunneling. As the collision energy increases, the agreement between QM and QCT DCSs improves, since the relative importance of tunneling contributions and other quantum effects decreases. At the highest collision energies, the QCT results account very well for the QM v' state-resolved DCSs for scattering angles larger than $\theta_{CM}=60°$.

As for the differences between the calculations on the SW and HSW PESs, apart from the smaller integral cross sections obtained in the latter PES (see above), the $v'=3$ forward peak is also smaller on the HSW PES for all collision energies studied. This can be expected from the higher barrier of the HSW PES as compared with the one of the SW PES.

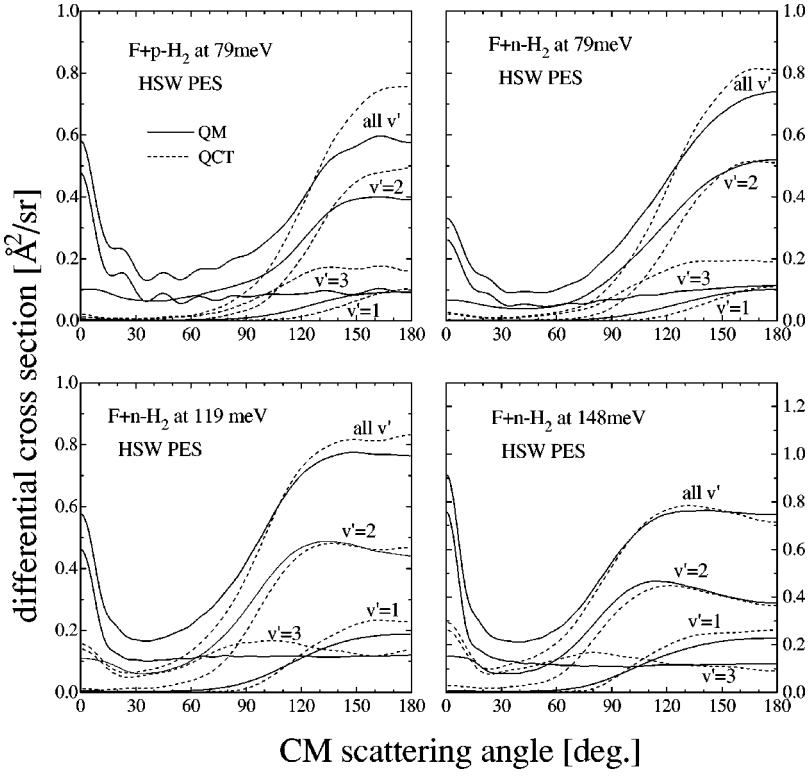

FIG. 2. Same as in Fig. 1 but for the HSW PES.

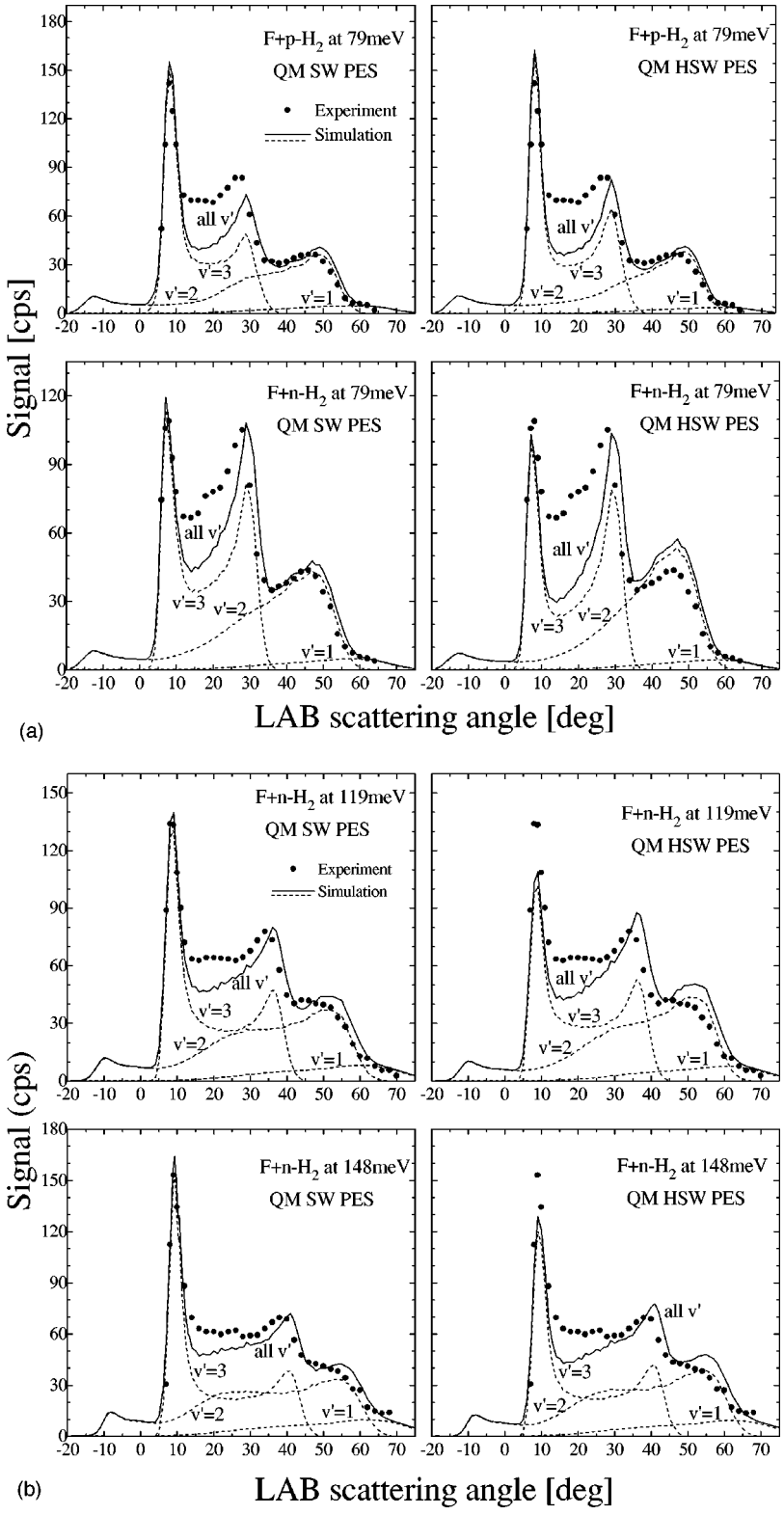

FIG. 3. Comparison between the experimental LAB ADs of Neumark *et al.* (Ref. 2) (solid points) and the theoretically simulated LAB ADs (solid line) using the QM v',j' state-resolved DCSs calculated on both the SW and HSW PESs as indicated. (a) $F+p-H_2$ and $F+n-H_2$ reactions at 79 meV collision energy. (b) $F+n-H_2$ at 119 and 148 meV. The dashed lines are the simulated contributions of the different v' states to the total LAB AD.

The simulation of the experimental LAB ADs of Neumark *et al.*[2] at the indicated collision energies using the present QM v',j' state-resolved DCSs calculated on both the SW and HSW PESs are portrayed in Figs. 3(a) and 3(b). The simulations carried out on the SW PES using the newly calculated DCSs are almost identical to those reported in Ref. 1. This is not surprising since the level of resolution of the LAB AD measurements of Ref. 2 does not allow the identification of the differences in the CM frame between the present results and those reported in Ref. 19 which have been commented on above. At the two highest collision energies, the experimental forward peak seems to be somewhat better accounted for by the new set of calculations on the SW PES. The simulations obtained using the DCSs calculated on the HSW PES do not represent a real improvement with respect to those on the SW PES, and in some instances, yield a

slightly worse agreement with the experimental LAB ADs. The $v'=3$ forward peak is underestimated at the two highest collision energies when using the calculations on the HSW PES. The lack of $v'=3$ sideways scattering, which was found to be the most important discrepancy between experiment and simulations based on calculations on the SW PES,[1] is still evident in the simulations based on the HSW PES. Overall, it seems that the inclusion of spin-orbit coupling in the calculation of the PES, with the consequent increase of the barrier height, yields results still not in full quantitative agreement with the experimental measurements. In any case, as discussed at length in a previous work,[1] except for a few details, most of the features of the experimental LAB ADs and time-of-flight (TOF) spectra are reproduced satisfactorily by the QM calculations on either of the two PESs. The corresponding simulations of the LAB AD using the QCT DCSs (not shown) are very similar to those presented in Ref. 1 and suffer from the absence of the necessary forward scattering into $v'=3$ to reproduce the experimental results, although the backward and sideways scattering are quite well accounted for on both PESs.

The experiment of Neumark *et al.*[2] has only vibrational resolution. It can be expected that the availability of experimental v',j' state-resolved DCSs can provide a more stringent test of the two PESs, as well as the possibility of revealing the presence of quantum mechanical effects. Keil and co-workers[10,11] have reported very recently new measurements of angular distributions for this reaction at a mean collision energy of 160 meV (3.69 kcal mol^{-1}), which essentially consist of the difference between the LAB ADs of two HF rovibrational states. As such, the experimental results have rotational resolution, although these angular distributions do not allow by themselves the determination of individual v',j' DCSs in the CM system. However, a (negative) bolometric signal at $\Theta_{LAB}\approx -8°$ was found corresponding to LAB angles which by kinematics could only correspond to HF $(v'=1,j')$ CM scattering into the forward hemisphere. Dharmasena *et al.* performed simulations of the experimental results using the QM $v'=1,j'$ and $v'=2,j'-1$ DCSs at the slightly different collision energy of 148 meV on the SW PES, provided by Castillo and Manolopoulos and based on the calculations of Ref. 19. The shape of the measured angular distributions were very well reproduced by the simulations including the above mentioned region of HF $(v'=1,j')$ CM forward scattering. Furthermore, in the simulations it was found that this forward scattering was mainly due to reaction with $H_2(j=1)$. Since the QCT calculations on this PES at 148 meV yielded practically no scattering into $v'=1$ at CM scattering angles below 60°,[14] the authors concluded that the presence of this $v'=1,j'$ forward scattering had to be a quantum mechanical effect.[10,11]

In the present work, new QM calculations have been performed for the title reaction on both the SW and HSW PESs at the collision energy of 160 meV. In addition, QCT calculations have been carried out at this same collision energy on both PESs in order to compare with the QM results. Figures 4(a) and 4(b) show the QM and QCT v' state-resolved DCSs on both PES for initial $j=0$ and $j=1$, respectively. For initial $j=0$, the agreement between QCT and QM DCSs on both PESs is only qualitative. Apart from the significantly smaller QCT forward scattering into $v'=3$ and $v'=2$, the backward scattering into $v'=1$ and $v'=2$ is also underestimated in the QCT case. The agreement improves notably for initial $j=1$ [see Fig. 4(b)], although the magnitude of the QCT forward peak is more than three times smaller than the QM one. It is interesting to notice that for CM angles below 50°, the scattering into $v'=1$ from QM and QCT calculations is very small on both PESs.

At this point, it is important to compare the theoretical v',j' state-resolved DCSs relevant for the experiment of Keil and co-workers. Figure 5 displays the QM and QCT CM DCSs for the $v'=1,j'=6$, and $v'=2,j'=5$ states for reaction from $H_2(j=1)$ calculated on both PESs, which are the states involved in the experimental $P_2(6)$ LAB AD of Refs. 10 and 11. As it can be seen, the agreement between the QM and QCT DCSs is good. Although in the QM $v'=1,j'=6$ DCSs there is some scattering into the forward hemisphere, it becomes very small for $\theta_{CM}<60°$. For $v'=2,j'=5$, the agreement between the QM and QCT DCSs is very good for scattering angles above 60°, and the main difference consists of the forward scattering at θ_{CM} below 30°, which is substantially smaller in the QCT case. Using the QM and QCT v',j' state-resolved DCSs, the $P_2(6)$ LAB AD has been simulated and the results are displayed in Fig. 6. As in the work of Dharmasena *et al.*, the different simulations have been independently normalized to the experiment at $\Theta_{LAB}=14°$. All the simulations based on QM or QCT results on both PESs clearly underestimate the negative peak at $\Theta_{LAB}\approx -8°$, as shown in the insert of Fig. 6. Although the forward scattering into $v'=1,j'=6$ is greater in the QM case, the difference between QM and QCT is much smaller than that between QM and experiment. The rest of the curve accessible experimentally is very well reproduced by the QM simulations on both PESs, and the comparison with the experiment does not allow us to discern between the SW and HSW PESs.

Figures 7 and 8 display the simulations of the experimental $P_2(5)$ LAB AD (involving the $v'=1,j'=5$ and $v'=2,j'=4$ states), and $P_2(7)$ LAB AD (involving the $v'=1,j'=7$ and $v'=2,j'=6$ states). The agreement between QM simulations and the experimental points is excellent in all angular regions with the exception of the negative peak at about $-8°$.

The conclusion to be drawn from these results is that QM calculations on neither of the two PESs can account for the $v'=1,j'=5,6,7$ scattering into the forward hemisphere revealed by the experimental measurements. The most obvious difference between the QM and QCT simulations is the smaller positive signal at LAB angles close to $\Theta_{LAB}=0°$, which corresponds to $v'=2,j'=4,5,6$ forward scattering. Unfortunately, this angular region was not accessible experimentally due to the proximity of the F atom beam. On the other hand, in the experiments of Neumark *et al.*,[2] no $v'=2$ forward scattering was found, whereas in the theoretical simulations of the LAB ADs there is a clear peak at $\Theta_{LAB}\approx -12°$ (see Fig. 3) caused by CM forward scattering into $v'=2$, which, in principle, would have to be experimentally detectable.

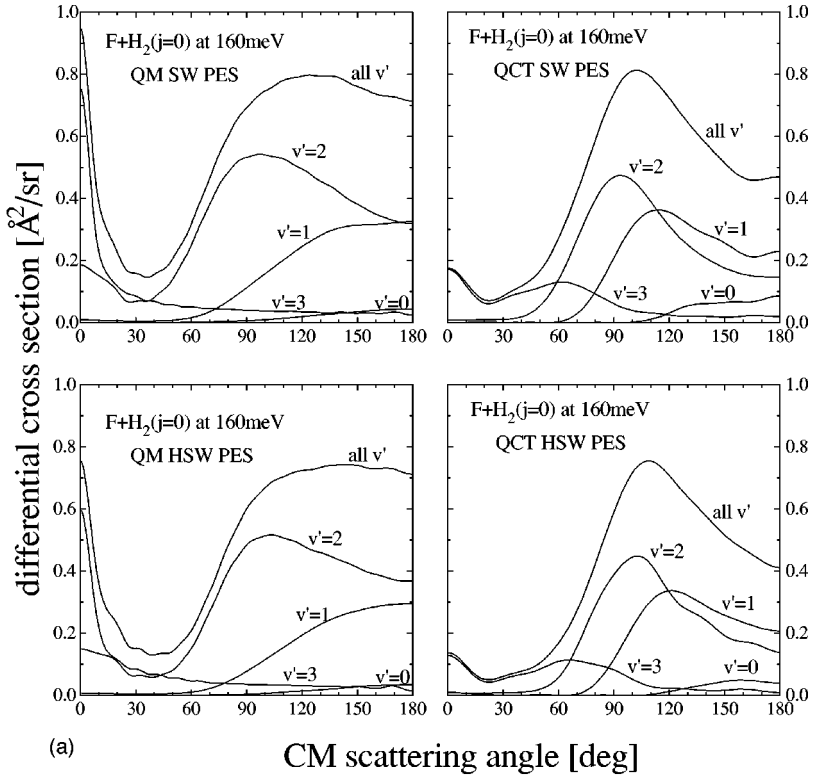

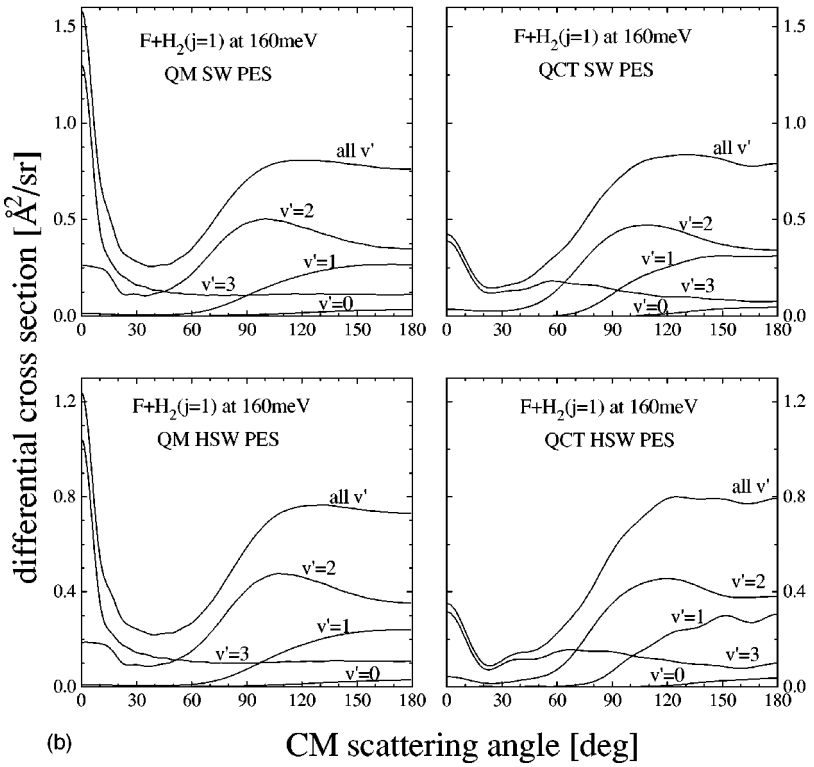

FIG. 4. QM and QCT v' state-resolved DCSs for the $F+H_2$ reaction at 160 meV collision energy calculated on both the SW and HSW PESs. (a) $F+H_2(j=0)$. (b) $F+H_2(j=1)$.

The availability of two PESs, which essentially differ on the height of the barrier located in the entrance channel, gives a good opportunity of investigating its effect in the magnitude of the conspicuous forward peak for $v'=3$ found in the present calculations and corroborated by the experiments of Neumark *et al.* The detailed analysis carried out by Castillo *et al.*[19] in terms of partial wave contribution to the forward scattering and the time delays of the peaks obtained in the cumulative reaction probability allowed them to conclude that the forward peak is caused by the highest angular momenta, and that it is dramatically enhanced with respect to the QCT one by tunneling through the combined centrifugal and potential energy barriers to reaction in the transition state region.

The present calculations carried out on the SW and HSW PESs seem to corroborate these conclusions. As shown

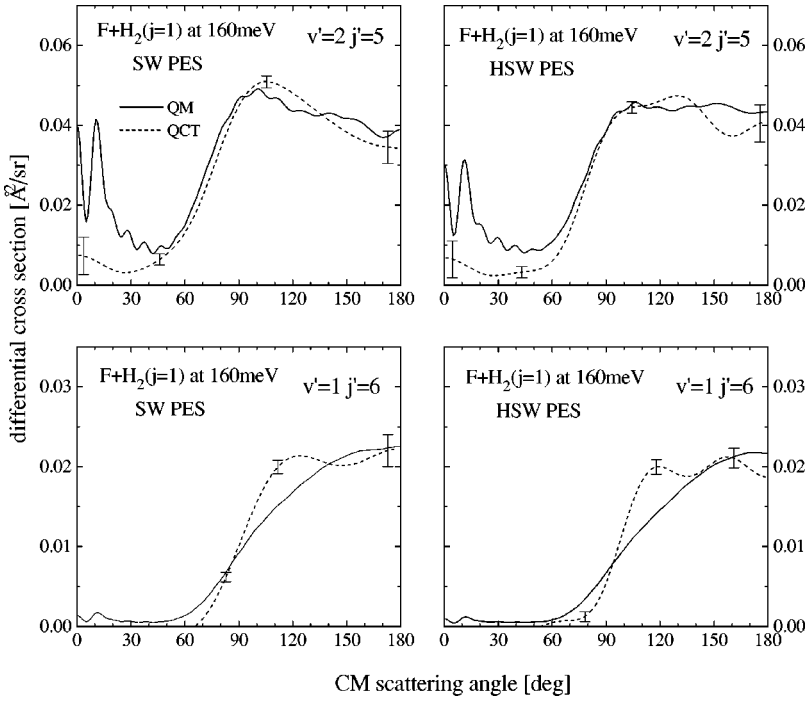

FIG. 5. QM (solid lines) and QCT (dashed lines) $v'=1, j'=6$ and $v'=2, j'=5$ state-resolved DCSs for the $F+H_2(j=1)$ reaction at 160 meV collision energy calculated on both the SW and HSW PESs.

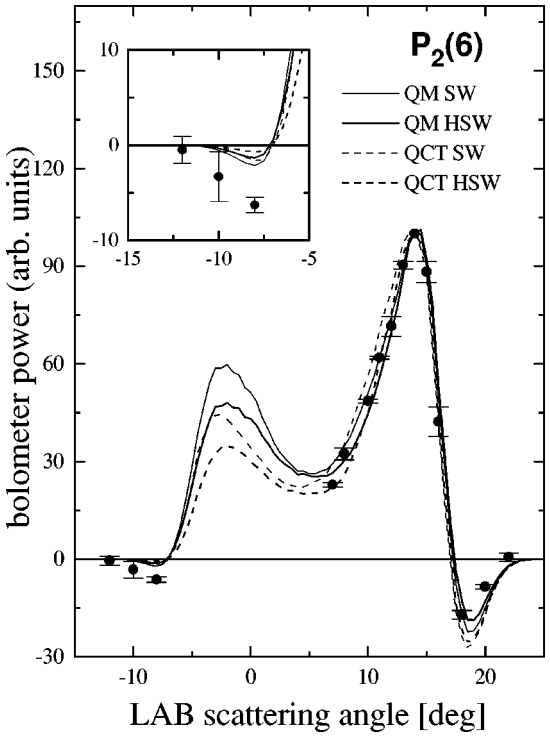

FIG. 6. Comparison between the experimental $P_2(6)$ LAB AD of Dharmasena *et al.* (Refs. 10 and 11) (solid points with error bars) and the theoretically simulated ones (solid and dashed lines) using the QM and QCT $v'=1, j'=6$ and $v'=2, j'=5$ state-resolved DCSs for the $F+H_2$ reaction at 160 meV collision energies calculated on both the SW and HSW PESs. The insert shows an amplification of the angular region between -15 and $-5°$ where the negative bolometer signal attributed to scattering into the forward hemisphere from the $v'=1, j'=6$ state of the HF product has been observed. As in Refs. 10 and 11, the scaling between experiment and the theoretical simulations has been made independently at the reference angle of $\Theta_{LAB}=14°$.

in Ref. 19, for initial $j=0$ the magnitude of the scattering into $v'=3$ at $\theta_{CM}=0°$ in the calculations on the SW PES remains practically invariant (about 0.75 $Å^2$/sr) and the forward peak becomes narrower as collision energy increases from 79 to 160 meV. For $j=1$ and 2 the height of the peak increases monotonically with collision energy from 0.3 $Å^2$/sr at 79 meV to 1.05 $Å^2$/sr at 160 meV. It is worth

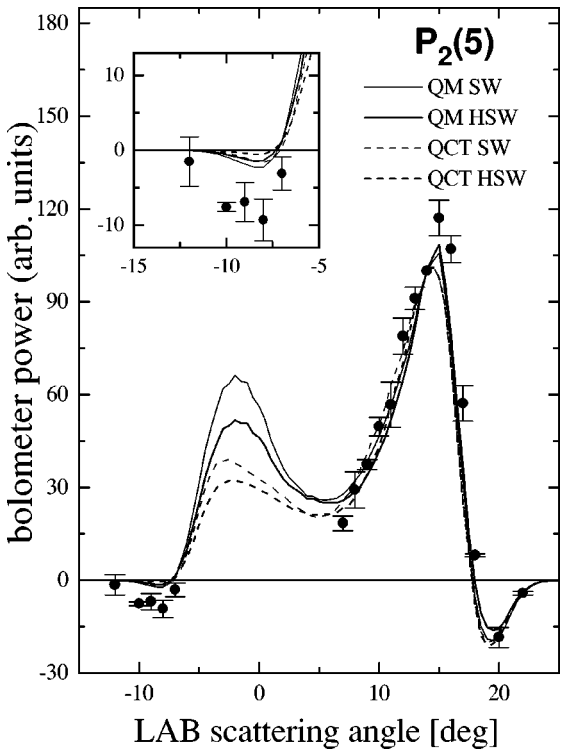

FIG. 7. As in Fig. 6, but for the $P_2(5)$ LAB AD.

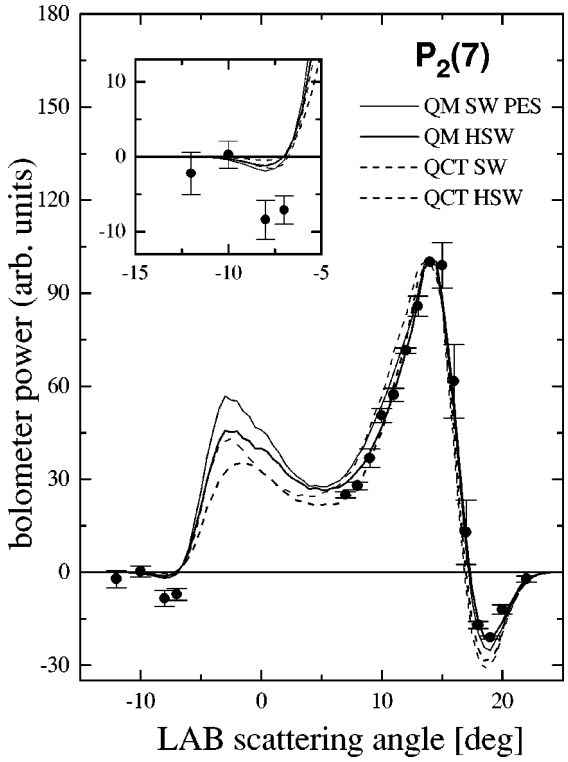

FIG. 8. As in Fig. 6, but for the $P_2(7)$ LAB AD.

noting that this effect is corroborated by the experimental LAB ADs of Neumark *et al.*; as shown in Fig. 3(a), the forward peak at 79 meV collision energy is considerably larger for the reaction with $p-H_2$ (80% $j=0$) than with $n-H_2$ (20% $j=0$, 74% $j=1$). In contrast, the QCT calculations on this PES show that the magnitude of the forward peak always increases with collision energy independently of initial j, and for $j=1$ is substantially larger than for $j=0$, although is smaller than in any of the QM calculations. The behavior on the HSW PES is entirely analogous except for the fact that for a given initial j and collision energy the scattering at $\theta_{CM}=0°$ is always smaller than in the SW PES.

Figure 9 shows the reaction probability as a function of the total angular momentum J, $P(J)$, calculated classically and quantum mechanically on the SW and HSW PESs for the $F+H_2(j=0)$ reaction at 160 meV collision energy. As expected, the QM reaction probability on the HSW PES decays more rapidly with increasing J, and the maximum total angular momentum for which there is reaction slightly decreases in comparison with the SW PES. A similar trend is found in the QCT calculations also shown in the figure. The comparison between the QM and QCT $P(J)$ shows that the maximum accessible J for reaction is noticeably smaller in the classical case than in the quantal one for a given PES.

As already discussed in Ref. 19, the forward peak is exclusively due to a narrow shell of J partial waves. As shown in Fig. 10, at $E_{coll}=160$ meV the QM $v'=3$ forward peak is almost completely produced by partial waves with $J>15$, and for $J>18$ up to $J=25$ only scattering contributions at $\theta<30°$ are obtained. This range of J constitutes a very well defined shoulder in the $P(J)$ peaking at $J=19$ and $J=18$ on the SW and HSW PESs, respectively (see Fig. 9). In the QCT case, the forward peak also consists of trajectories with $J>15$, but in contrast with the QM case, most of the trajectories with J between 15 and 18 contribute to increase the sideways scattering from 30 to 70° (see bottom panel of Fig. 10), which becomes markedly larger than the QM one, giving rise to a hotter rotational distribution than that found in the QM calculation.

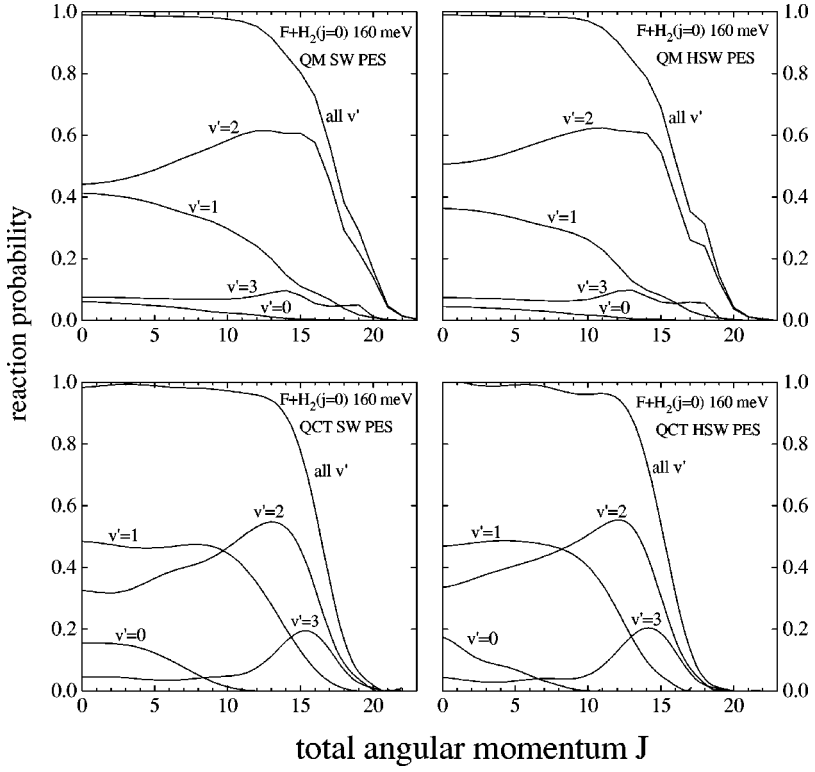

FIG. 9. QM and QCT reaction probabilities as a function of the total angular momentum J for the $F+H_2(j=0)$ reaction at 160 meV collision energy calculated on both the SW and HSW PESs.

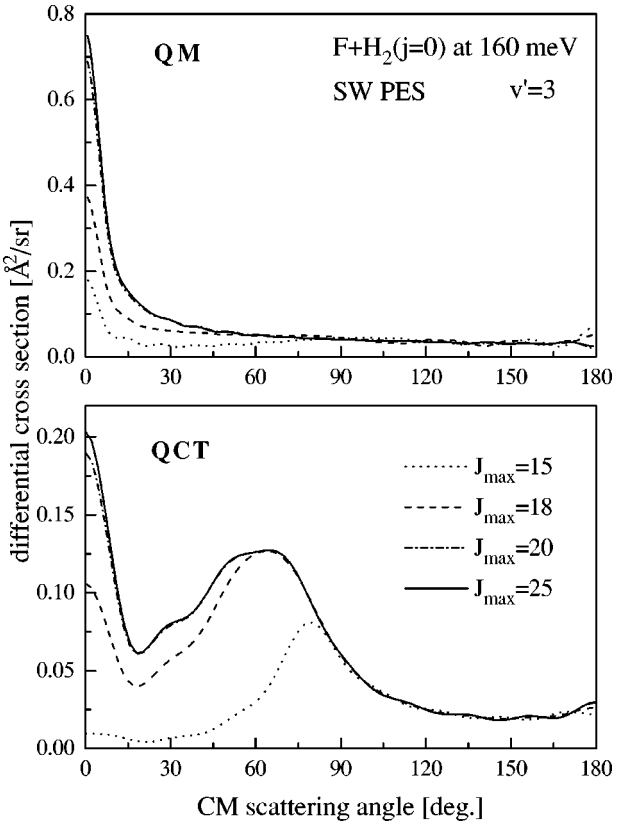

FIG. 10. QM (top panel) and QCT (bottom panel) DCSs for the $F+H_2(j=0)\rightarrow HF(v'=3)+H$ reaction resolved into different intervals of the total angular momentum (indicated as J_{max}) calculated on the SW PES. Notice that in both the QM and QCT calculations most of the forward scattering comes from J values within the interval 15 to 25. Notice also the very different scale of the abscissa in both panels; the scattering at $\theta<30°$ from the QM calculation is about four times larger than that obtained in the QCT calculation.

It is interesting to note that the reaction probability into $v'=2$ is larger than that for $v'=3$, especially at high values of J, and that the largest Js accessible for reaction yield products into $v'=2$ rather than into $v'=3$. The analysis of the QM $v'=2$ forward scattering indicates, however, that it is originated by strong interferences from a very wide range of J values, and, whereas the $v'=3$ forward peak is rotationally very cold ($j'=0-2$), as shown in Fig. 11, the forward scattering into $v'=2$ contains contributions of larger j'.

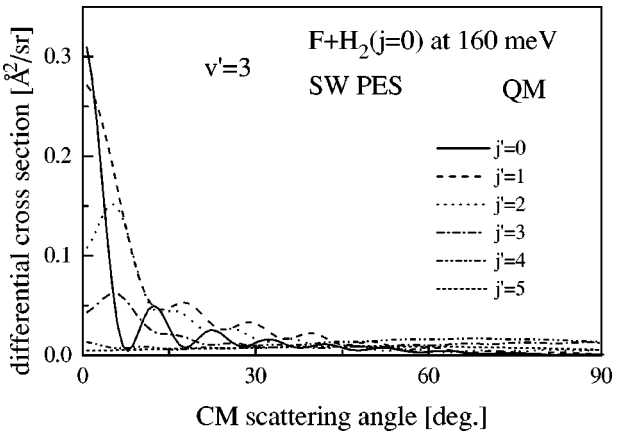

FIG. 11. QM DCSs for the $F+H_2(j=0)\rightarrow HF(v'=3, j')+H$ calculated on the SW PES at 160 meV collision energy.

IV. CONCLUSIONS

New thorough quantum mechanical (QM) and quasiclassical trajectory (QCT) calculations have been carried out for the $F+H_2$ reaction at the experimental collision energies and H_2 rotational quantum numbers $j=0-2$ on the SW PESs, and on the new HSW PES which takes into account the spin-orbit interaction in the entrance valley. The QM results on the SW PESs differ from those already published by Castillo *et al.*,[19] since more projections of the total angular momentum into the body-fixed axis have been taken into account, therefore improving the convergence of the calculations. The theoretical results have been used to simulate the experimental laboratory (LAB) angular distributions (AD) measured by Lee and co-workers[2] and Keil and co-workers.[10,11]

The simulations of the LAB ADs of Neumark *et al.*[2] carried out using the new QM calculations on the SW PES yield a similar degree of agreement with the experimental results than those reported in a previous work.[1] The QM and QCT calculations on the new HSW PESs, which has a larger barrier, yield significant less forward scattering than those on the SW PES, since less partial waves contribute to the reaction. The QM simulations carried out on this new PES do not improve, and in some instances even worsen, the agreement with the experimental results.

The QCT and QM simulations on both the SW and HSW PES of the rovibrational LAB ADs obtained by Dharmasena *et al.*[10,11] are in good agreement with the experimental results, except for the negative bolometric signal assigned to forward scattering in the center-of-mass (CM) frame into the individual HF ($v'=1,j'=5,6,7$) states. The new calculations presented here do not yield a significant scattering in that angular region.

In spite of the success of the theoretical calculations in reproducing most of the experimental findings, none of the dynamical calculations on the *ab initio* PESs here studied is capable of accounting for all the details found in the experimental measurements. In particular, the above mentioned forward scattering into HF ($v'=1,j'$) experimentally evidenced is not reproduced by the theoretical calculations. A better agreement with the angular distributions of Lee and co-workers clearly requires more sideways scattering into HF ($v'=3$), which is not found in the QM calculations. There are some hints that nonadiabatic processes might play a significant role for this reactive system.[9,29,30] Future theoretical calculations involving different surfaces coupled nonadiabatically will shed light on this point.

ACKNOWLEDGMENTS

We are indebted to David Manolopoulos for his help and support to carry out this work. B.M-H. acknowledges financial support through the program ''Acciones para la incorporación de doctores y tecnólogos'' of the Ministry of Education and Culture of Spain. J.F.C. acknowledges the EPSRC for the award of a postdoctoral research position in Oxford.

The Spanish contribution to this work was financed by the DGICYT under Project No. PB95-0918-C02. The German part of this work received generous funding from the German Fonds der Chemischen Industrie. The Spanish–German exchange program ''Acciones Integradas'' is also acknowledged.

[1] F. J. Aoiz, L. Bañares, B. Martínez-Haya, J. F. Castillo, D. E. Manolopoulos, K. Stark, and H.-J. Werner, J. Phys. Chem. A **101**, 6403 (1997).
[2] D. M. Neumark, A. M. Wodtke, G. N. Robinson, C. C. Hayden, and Y. T. Lee, J. Chem. Phys. **82**, 3045 (1985).
[3] K. Stark and H.-J. Werner, J. Chem. Phys. **104**, 6515 (1996).
[4] M. Faubel, B. Martínez-Haya, L. Y. Rusin, U. Tappe, and J. P. Toennies, Chem. Phys. Lett. **232**, 197 (1995).
[5] M. Faubel, B. Martínez-Haya, L. Y. Rusin, U. Tappe, J. P. Toennies, F. J. Aoiz, and L. Bañares, Chem. Phys. **207**, 227 (1996).
[6] M. Baer, M. Faubel, B. Martínez-Haya, L. Y. Rusin, U. Tappe, J. P. Toennies, K. Stark, and H.-J. Werner, J. Chem. Phys. **104**, 2743 (1996).
[7] M. Faubel, B. Martínez-Haya, L. Y. Rusin, U. Tappe, and J. P. Toennies, J. Phys. Chem. A **101**, 6415 (1997).
[8] M. Baer, M. Faubel, B. Martínez-Haya, L. Y. Rusin, U. Tappe, and J. P. Toennies, J. Chem. Phys. **108**, 9694 (1998).
[9] W. B. Chapman, B. W. Blackmon, and D. J. Nesbitt, J. Chem. Phys. **107**, 8193 (1997).
[10] G. Dharmasena, T. R. Phillips, K. N. Shokhirev, G. A. Parker, and M. Keil, J. Chem. Phys. **106**, 9950 (1997).
[11] G. Dharmasena, K. Copeland, J. H. Young, R. A. Lasell, T. R. Phillips, G. A. Parker, and M. Keil, J. Phys. Chem. A **101**, 6429 (1997).
[12] F. J. Aoiz, L. Bañares, M. Faubel, B. Martínez-Haya, L. Y. Rusin, U. Tappe, and J. P. Toennies, Chem. Phys. **207**, 245 (1996).
[13] P. Honvault and J. M. Launay, Chem. Phys. Lett. **287**, 270 (1998).
[14] F. J. Aoiz, L. Bañares, V. J. Herrero, V. Sáez Rábanos, K. Stark, and H.-J. Werner, Chem. Phys. Lett. **223**, 215 (1994).
[15] B. Hartke and H.-J. Werner, Chem. Phys. Lett. **280**, 430 (1997).
[16] S. E. Bradforth, D. W. Arnold, D. M. Neumark, and D. E. Manolopoulos, J. Chem. Phys. **99**, 6345 (1993).
[17] D. E. Manolopoulos, K. Stark, H.-J. Werner, D. W. Arnold, S. E. Bradforth, and D. M. Neumark, Science **262**, 1852 (1993).
[18] C. L. Russell and D. E. Manolopoulos, Chem. Phys. Lett. **256**, 465 (1996).
[19] J. F. Castillo, D. E. Manolopoulos, K. Stark, and H.-J. Werner, J. Chem. Phys. **104**, 6531 (1996).
[20] H.-J. Werner and P. J. Knowles, J. Chem. Phys. **89**, 5803 (1988).
[21] MOLPRO is a package of *ab initio* programs written by H.-J. Werner and P. J. Knowles, with contributions from R. D. Amos, A. Berning, D. L. Cooper, M. J. O. Deegan, A. J. Dobbyn, F. Eckert, C. Hampel, T. Leininger, R. Lindh, A. W. Lloyd, W. Meyer, M. E. Mura, A. Nicklass, P. Palmieri, K. Peterson, R. Pitzer, P. Pulay, G. Rauhut, M. Schütz, H. Stoll, A. J. Stone, and T. Thorsteinsson.
[22] Files with the FORTRAN codes of both surfaces can be downloaded from http://www.theochem.uni-stuttgart.de/research/h2fpots.
[23] D. E. Manolopoulos and J. F. Castillo (to be published).
[24] F. J. Aoiz, V. J. Herrero, and V. Sáez Rábanos, J. Chem. Phys. **97**, 7423 (1992).
[25] V. M. Azriel, G. D. Billing, L. Yu. Rusin, and M. B. Sevryuk, Chem. Phys. **195**, 243 (1995).
[26] F. J. Aoiz, L. Bañares, V. J. Herrero, V. Sáez Rábanos, K. Stark, and H.-J. Werner, J. Chem. Phys. **102**, 9248 (1995).
[27] J. E. Pollard, D. J. Trevor, Y. T. Lee, and D. A. Shirley, J. Chem. Phys. **77**, 4818 (1982).
[28] D. E. Manolopoulos, J. Chem. Soc., Faraday Trans. **93**, 673 (1997), and references therein.
[29] M. Faubel, L. Y. Rusin, F. Sondermann, S. Schlemmer, U. Tappe, and J. P. Toennies, J. Chem. Phys. **101**, 2106 (1994).
[30] M. Faubel, B. Martínez-Haya, L. Y. Rusin, U. Tappe, and J. P. Toennies, Z. Phys. Chem. (Munich) **188**, 197 (1995).